Quantitative elemental analysis of specimens in-air via External Beam Particle Induced X-ray Emission with a compact laser-driven proton source

Martina Salvadori,[1, *] Fernando Brandi,[1, †] Luca Labate,[1, ‡] Federica Baffigi,[1] Lorenzo Fulgentini,[1]
Pietro Galizia,[2] Petra Koester,[1] Daniele Palla,[1] Diletta Sciti,[2] and Leonida A. Gizzi[1, §]

[1]*Consiglio Nazionale delle Ricerche, Istituto Nazionale di Ottica (CNR-INO), Pisa, Via Moruzzi, 1, 56124 Pisa, Italy.*
[2]*Consiglio Nazionale delle Ricerche, Istituto di Scienza,*
Tecnologia e Sostenibilità per lo Sviluppo dei Materiali Ceramici (CNR-ISSMC), Faenza, Italy.
(Dated: November 19, 2023)

Particle Induced X-ray Emission (PIXE) is a well established ion beam analysis technique, enabling quantitative measurement of the elemental composition of a sample surface. Electrostatic accelerators are today used as proton beam sources in PIXE systems, restricting its feasibility to relatively large scale facilities. We present a novel PIXE technique based on a compact laser-driven proton accelerator with the sample in ambient atmosphere, which simplifies the measurements, and is strictly necessary for those samples that cannot sustain vacuum environment. It features a 10 TW class ultrashort laser, used to generate a few MeV proton beam, and a compact proton transport magnetic beamline, acting also to prevent unwanted fast electrons from reaching the sample. An X-ray CCD camera used in single photon detection is used to retrieve the spectrum of the radiation emitted by the samples upon irradiation in air. Quantitative elemental composition analysis is performed and validated against standard Energy-dispersive X-ray spectroscopy measurements, showing the feasibility of External Beam PIXE analysis with compact laser-driven accelerators.

Ultraintense pulsed laser-matter interaction for proton acceleration has been studied for more than two decades and is nowadays well understood theoretically, numerically described by reliable models, as well as routinely implemented in many research laboratories worldwide [1–3]. Appealing features of laser-driven particle accelerators include their very compact footprint, and the intrinsically short bunch duration. Historically, proton beams with energy up to several tens of MeV have first been reported using large-scale, high-energy ($\sim 10\,\mathrm{J}$) laser systems, whose repetition rate is usually limited to a fraction of Hz. Acceleration of protons is achieved through the so-called Target Normal Sheath Acceleration (TNSA) process [4–6]; in this process, populations of fast (up to the MeV range) electrons are accelerated at the laser critical surface on the front side of a thin solid target, which then propagate through the overdense target and, on exiting the rear surface, induce a strong electric field (up to TV/m), thereby accelerating protons and light ions. Over the past decade or so, ultrashort and ultraintense laser pulses have also been used to the purpose [7–9], with the added value of allowing, in principle, high repetition rate (i.e., high average flux) beams to be produced; furthermore, novel proton acceleration regimes, based on phenomena such as Relativistic Induced Transparency and/or Radiation Pressure Acceleration[10–12] have been found to enable the acceleration of beams with $\gtrsim 100\,\mathrm{MeV}$ energy. This kind of study have been carried out using 100 TW class laser systems.

On the other hand, few MeV proton beams can be efficiently accelerated, via TNSA, with smaller scale, 10 TW class lasers. Such sources can in principle provide an alternative to the usage of conventional proton accelerators (TANDEM, cyclotrons, etc.), with appealing features such as, for instance, the reduced requirements on the ionizing radiation shielding, made possible by the acceleration processes taking place over very small distances. In general, given the maturity and potential of laser-driven particle acceleration, much effort is currently devoted to seek for actual implementations of laser-driven compact accelerators, of either electrons or protons/light ions, in real practical applications beyond basic research and proof-of-principle experiments. Notable examples span from large international projects aiming at high quality electron accelerators facilities [13], to the very rapidly growing interest in novel radiotherapy protocols based by laser-driven accelerators [14–16].

Few MeV proton beams are well suited for nondestructive analysis via Particle Induced X-ray Emission (PIXE), which is a well established technique used to characterize quantitatively the elemental composition of a sample surface through the spectral analysis of the characteristic X-ray radiation generated upon particle irradiation [17–20]. A very relevant specificity of PIXE technique is the possibility to perform the sample irradiation in ambient atmosphere by letting the proton beam propagate in air, i.e., *External Beam* PIXE. This approach has several advantages and greatly simplify the implementation of PIXE, by speeding up the analysis of a large amount of samples [21, 22], and by reducing sample charging and heating, therefore minimizing possible damages of delicate specimens. Notably, external beam PIXE is *strictly necessary* in those cases where samples cannot sustain vacuum environment or be placed inside a vacuum chamber [23–27].

---

* martina.salvadori@ino.cnr.it
† fernando.brandi@ino.cnr.it
‡ luca.labate@ino.cnr.it; Also at Istituto Nazionale di Fisica Nucleare (INFN), Sezione di Pisa, Italy.
§ Also at Istituto Nazionale di Fisica Nucleare (INFN), Sezione di Pisa, Italy.

Today PIXE systems are based on electrostatic proton accelerators, restricting the feasibility of such analysis to medium-to-large scale facilities. There is however a growing interest in developing smaller scale PIXE systems, for example based on a 2 MeV RF-driven compact accelerators [28]. The use of laser-driven few MeV proton accelerators for PIXE is extremely appealing and it has been recently investigated theoretically through modelling and simulations [29–33], as well as with experiments employing relatively high power laser systems with the samples in vacuum [34–36].

Here, we introduce the External Beam Laser-PIXE (EBL-PIXE) technique and report about the development, characterisation and validation of a practical system based on a relatively simple design comprising: i) a compact few MeV TNSA-based proton source; ii) an efficient magnetic quadrupole beam line used to transport the protons from the source to air; iii) a CCD camera in single photon detection used for the spectral analysis of the X-ray emitted by the sample under investigation. The performances of EBLaser-PIXE are assessed firstly in terms of the characteristics and stability of the laser-driven proton beam, and then with actual PIXE measurements on multi-element sample validated through quantitative comparison with standard Energy-Dispersive X-ray Spectroscopy (EDS) analysis.

The schematic representation of the compact EBL-PIXE system is reported in Fig. 1 and a picture of the irradiation site in air is shown as inset. The Ti:Sapphire 14 TW 10 Hz beamline at the Intense Laser Irradiation Laboratory of the CNR-INO in Pisa [37] is used to drive the TNSA-based proton source. The laser beam was focused down to a $\sim 3\,\mu$m FWHM spot size using an $f/ \sim 1.5$ Off-Axis Parabola (OAP), at an intensity $\sim 4 \times 10^{19}$ Wcm^{-2}, see Supplementary Material (SM) for technical details. A $5\,\mu$m thick titanium foil was used as a target, to accelerate proton beams via the TNSA process. In the present measurements the target position was refreshed after each laser shot with a maximum frequency of $\sim 0.1\,$Hz, limited by the target movement and alignment system; rep rate operation up to 10 Hz are feasible with a rapidly moving foil like for example a rolling tape target [38, 39]. The laser-driven proton beam propagates in the direction normal to the rear surface of the target with a divergence $\sim 15°$ HWHM, typical of few MeV TNSA proton beams [40–42]. In order to efficiently transport the protons from the source to the application site a Magnetic Beamline (MBL) can be used [43–45]. For EBL-PIXE we have designed a modular and cost effective MBL composed of a sequence of magnetic quadrupoles based on commercial neodymium permanent magnets of 25x12x4 mm^3 dimensions, embedded in soft iron supporting cages. The first two quadrupoles facing the TNSA-target are designed with a 25x25 mm^2 clear aperture, while the others have 12x12 mm^2 clear aperture. The MBL was placed at 12.5 mm from the proton source, it is 24.9 cm long, and the quadrupoles orientation is alternating along the line, as shown in Fig. 2(a). In order to allow
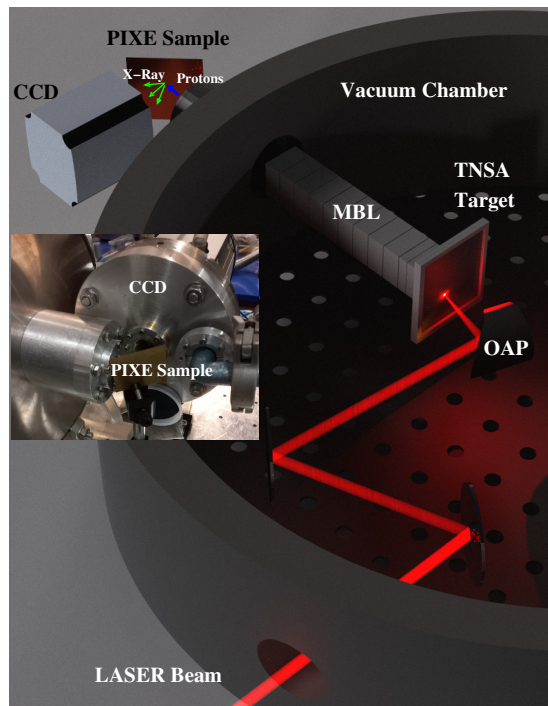

FIG. 1. Representation of the EBL-PIXE system showing the main components (not to scale): the TW laser beam, the Off-Axis Parabolic mirror (OAP), the Magnetic Beamline (MBL), the PIXE Sample and the X-ray CCD; the proton beam and the X-ray are represented by blue and green arrows respectively; the TNSA proton source and the MBL are contained in a vacuum chamber, the PIXE sample is in air, and the CCD chip is kept in vacuum environment; the inset shows a picture of the actual EBL-PIXE irradiation site.

a proton beam optimization and characterization without any transport, the MBL was moved in and out of the beam path via a motorized stage. The transported proton beam was finally let in ambient atmosphere through a 13-micron thick circular Kapton window. The PIXE sample was placed in ambient atmosphere at 2 cm from the Kapton window with the surface oriented at 45° with respect to the MBL axis, as shown in Fig. 1. The spectrum of the X-ray emitted by the sample upon proton irradiation was measured shot-by-shot by a CCD camera (ANDOR, IKON-M) acquiring in single-photon regime [49] and placed at 90° with respect to the MBL axis, as shown in Fig. 1. The analysis to retrieve the energy spectrum from the raw CCD acquisitions was carried out using the procedure described in [50]. Further details on the CCD setup can be found in the SM; here we only mention that the low energy cut-off of our spectral measurement device was of about 5 keV.

The MBL performance was studied with Monte Carlo simulations based on the GEANT4 toolkit [46, 47], as described in [48]. The transverse view of the simulated proton beam is reported in Fig. 2(a). The proton source used in the simulations is described by a TNSA-like decreasing exponential energy spectrum with a sharp cutoff

at 3 MeV, as from the data obtained experimentally. The resulting cross-section profile of the proton beam in air is reported in the left panel of Fig. 2(b). For comparison the cross-section profile of the proton beam in air simulated w/o the MBL is shown in the right pannel of Fig. 2(b). The calculated enhancement factor of the integrated flux per shot with the MBL compared with the case w/o MBL is ∼7. Notably, the MBL had also the fundamental effect of removing the TNSA fast electrons from the proton beam path, which is absolutely necessary for quantitative PIXE analysis since the interaction of such fast electrons with the sample also efficiently generates X-ray emission; this would result in a significant spurious contribution to the total X-ray signal. In Fig. 2(c) a GEANT4 simulation showing the complete damping of the laser-driven electrons is reported. In this simulation, we assumed a fast electron beam having an exponential energy distribution, with a temperature $T_{fe} \simeq 1.5$ MeV, as provided by the well consolidated scaling law $T_{fe} = m_e c^2(\sqrt{1 + a_0^2/2} - 1)$ where $a_0 = 0.85(I[10^{18}\text{Wcm}^{-2}]\lambda^2[\mu m])^{1/2}$ is the normalized vector potential [51].

The energy spectrum of the proton beam was characterized using a Thomson Parabola Spectrometer (TPS)[8, 52, 53] while the high energy cut-off of the beam transported in air was monitored with a Time-of-Flight (ToF) measurement using a Si-PIN detector [48]. A typical TPS measurement data of the laser-driven particle source in vacuum is shown in Fig. 3(a), where the proton parabolic trace is the lower one. Visible in Fig. 3(a) are also the parabolic traces of the ions which are all stopped by the Kapton window when irradiation in air is performed. In Fig. 3(b) the proton source energy spectrum as obtained from the TPS measurements is shown. The long term stability of the high-energy cut-off of the proton beam was monitored with ToF measurements in air over tens of shots, as shown in Fig. 3(c). It must be noted that the TPS employing a micro-channel plate intensifier is more sensitive compared to the ToF measurement based on solid state detectors, thereby leading to the slightly higher estimate for the cut-off energy. The two measurement set indicate a high-energy cut-off stably around 3 MeV. During sample irradiation with external beam all protons from the laser-driven source with energy smaller than 1.3 MeV were stopped in the Kapton window plus the 2 cm of air, as calculated using SRIM software [54]. The total proton flux at the sample position in air was measured by means of unlaminated EBT3 radiochromic films (see SM). In the left panel of Fig. 3(d) the image of the EBT3 film irradiated with a single shot using the MBL is shown. The integrated proton number over the beam cross section is estimated to be ∼ 10^7 per shot. For comparison, the image of the EBT3 irradiated with 10 shots without using the MBL is reported in the right pannel of Fig. 3(d). The observed circular shape in the exposed EBT3 films is due to the Kapton window used as vacuum-air interface. The experimentally measured enhancement flux factor with and w/o MBL is ∼8, in good
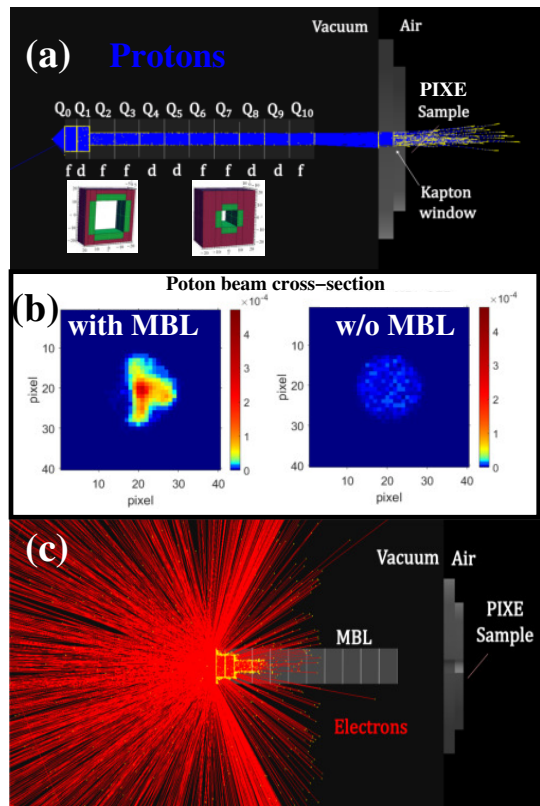

FIG. 2. The MBL design and characteristics: (a) MBL schematic with the PIXE sample location indicated and the simulated proton beam transport; the notation "f" and "d" indicates the alternating orientation of the magnetic field in the eleven quadrupoles denoted by Q_i, $i = 0$ to 10; the schematic of the two quadrupole magnet types are shown in the two insets. (b) Cross section distribution of the simulated proton beam at the PIXE sample location in air with and w/o MBL, left and right pannel respectively, where a pixel area corresponds to 1 mm^2; the circular shape of the simulated beam is due to the Kapton window used as vacuum-air interface. (c) Simulation of propagation in the MBL of the fast electrons from the laser-driven source.

agreement with the Monte Carlo transport simulations.

In order to quantitatively assess the EBL-PIXE measurements, an elemental analysis of a brass (Copper-Zinc alloy) sample was performed. Fig. 4(a) shows the X-ray spectrum obtained summing up the signal over 39 laser shots, after correction for the X-ray attenuation and for the CCD quantum efficiency (see SM). We first observe that the linewidth of the X-ray line peaks is about few hundreds eV; this is comparable to the ones obtained with standard PIXE measurements carried out with electrostatic accelerators and silicon drift detectors [20], and it allows to resolve the K$_\alpha$ and K$_\beta$ emission lines. The result of a non-linear fit used to analyse the data points is also shown in Fig.4(a). The fit is performed using Gaussian functions with a background estimated from a quadratic fit on the data points preceding the actual X-ray lines. As typical in PIXE measurements, the K$_\alpha$ line
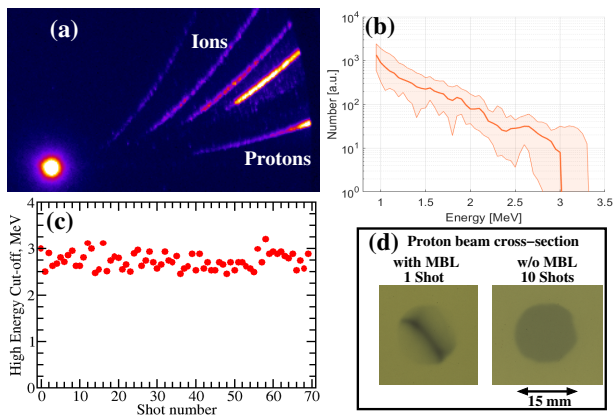
FIG. 3. Characterization of the laser-driven proton beam. (a) Typical TPS data, with the proton parabolic trace in the lower right; the traces of the ions are also visible. (b) Proton beam spectrum as from the TPS proton traces. (c) Proton beam high energy cut-off estimated by ToF measurements. (d) Proton beam cross-section measured with EBT3 films with and w/o MBL, left and right pannels respectively.

area was considered as a measure of the X-ray yield Y used for the analysis, and its ratio between Cu and Zn is found to be $Y_{Cu}/Y_{Zn} = 2.62$ with an estimated uncertainty of about 10%.

The ratio of the percentage atomic density from the EBL-PIXE measurement is calculated using the ratio of the X-ray yield normalized to the proton induced K-shell emission cross-section σ_{Cu} and σ_{Zn}. The values for this last quantity are taken from the reference manuscript by Paul and Sacher [55]; their ratio is very slowly varying in the few MeV range(see SM). For the final calculation, a value of $\sigma_{Cu}/\sigma_{Zn} = 1.21$ and an uncertainty of ± 0.07 are considered. The actual quantitative elemental composition obtained by the EBL-PIXE measurement is then calculated from the ratio

$$\frac{N_{PIXE,Cu}}{N_{PIXE,Zn}} = \frac{Y_{Cu}}{Y_{Zn}} \times \frac{\sigma_{Zn}}{\sigma_{Cu}}, \qquad (1)$$

and assuming Cu and Zn are the only constituents of the sample, as confirmed also by the EDS measurement. The final sample composition is $N_{PIXE,Cu} = 68.4\%$ and $N_{PIXE,Zn} = 31.6\%$ with an uncertainty of 3.5%.

The result of the EDS analysis of the brass sample after 15 measurements is reported in Fig. 4(b), resulting in the atomic density percentage of $N_{EDS,Cu} = 69.1\%$ and $N_{EDS,Zn} = 30.9\%$ with an uncertainty of 1% (see SM). The comparison of the elemental composition of the brass sample measured by the EBL-PIXE and EDS techniques is summarized in Table I, showing a very good agreement between the two measurements.

In summary, we have implemented and validated for the first time to our best knowledge the External Beam Laser-PIXE technique for nondestructive elemental analysis of specimens in air. The analysis was performed with a few tens of laser shots by recording the X-ray spectra using a CCD camera in single photon acquisition. The
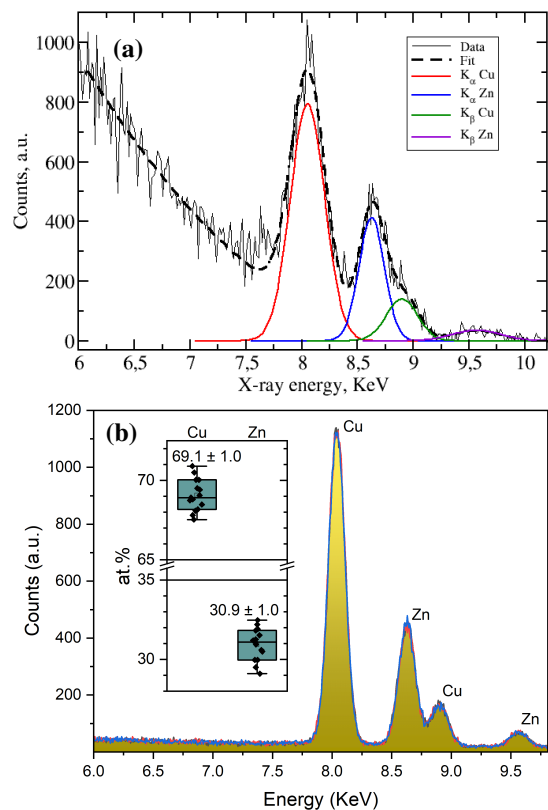

FIG. 4. (a) EBL-PIXE spectrum of the brass sample, showing the results of the fit on the data points and the resulting Gaussian functions for the copper and zinc K_α and K_β lines. (b) Results of the EDS analysis of the brass sample.

TABLE I. Elemental composition of the brass sample from EBL-PIXE and EDS measurements.

Technique	Copper, %	Zinc, %
EBL-PIXE	68.4(3.5)	31.6(3.5)
EDS	69.1(1.0)	30.9(1.0)

driving pulsed laser system can run up to 10 Hz repetition rate, meaning that PIXE measurement can be performed within seconds of irradiation employing a fast moving laser-plasma target. For comparison, fast standard PIXE measurement can typically take up to minutes [56]. The quantitative elemental analysis was compared against standard EDS measurements in vacuum, and a very good agreement was found. The present demonstration of a novel, accurate and easy to operate nondestructive analysis methodology based on laser-driven particle accelerators will stimulate further implementation of laser-driven accelerators in real practical applications.

[1] H. Daido, M. Nishiuchi, and A.S. Pirozhkov, Review of laser-driven ion sources and their applications Rep. Prog. Phys. **75**, 056401 (2012).

[2] A. Macchi, M. Borghesi, and M. Passoni, Ion acceleration by superintense laser-plasma interaction Rev. Mod. Phys. **85**, 751 (2013).

[3] J. Schreiber, P.R. Bolton, and K. Parodi, "Hands-on" laser-driven ion acceleration: A primer for laser driven source development and potential applications, Rev. Sci. Instrum. **87**, 071101 (2016).

[4] R.A. Snavely, M.H Key, S.P. Hatchett, T.E. Cowan, M. Roth, T.W. Phillips, M.A. Stoyer, E.A. Henry, T.C. Sangster, M.S. Singh, *et al.*, Intense High-Energy Proton Beams from Petawatt-Laser Irradiation of Solids, Phys. Rev. Lett. **85**, 2945 (2000).

[5] S.C. Wilks, A.B. Langdon, T.E. Cowan, M. Roth, M. Singh, S. Hatchett, M.H. Key, D. Pennington, A. MacKinnon, and A.R. Snavely, Energetic proton generation in ultra-intense laser–solid interactions, Phys. Plasmas, **8**, 542 (2001).

[6] L.A. Gizzi, D. Giove, C. Altana, F. Brandi, P. Cirrone, G. Cristoforetti, A. Fazzi, P. Ferrara, L. Fulgentini, P. Koester, *et al.*, A New Line for Laser-Driven Light Ions Acceleration and Related TNSA Studies, Appl. Sci. **7**, 984 (2017).

[7] T. Ziegler *et al.*, Proton beam quality enhancement by spectral phase control of a PW-class laser system, Sci. Rep. **11**, 7338 (2021)

[8] L.A. Gizzi, E. Boella, L. Labate, F. Baffigi, P.J. Bilbao, F. Brandi, G. Cristoforetti, A. Fazzi, L. Fulgentini, D. Giove, *et al.*, Enhanced laser-driven proton acceleration via improved fast electron heating in a controlled preplasma, Sci. Rep. bf 11, 13728 (2021).

[9] M. Rehwald, *et al.*, Ultra-short pulse laser acceleration of protons to 80 MeV from cryogenic hydrogen jets tailored to near-critical density, Nat. Comm. **14**, 4009 (2023)

[10] C. A. J. Palmer *et al.*, Monoenergetic proton beams accelerated by a radiation pressure driven shock, Phys. Rev. Lett. **106**, 014801 (2011)

[11] A. Higginson *et al.*, Near-100 MeV protons via laser-drfiven transparency-enhanced hybrid acceleration scheme, Nat. Comm. **9**, 724 (2018)

[12] A. Henig *et al.*, Enhanced laser-driven ion acceleration in the relativistic tranparency regime, Phys. Rev. Lett. **103**, 045002 (2009)

[13] R. W. Assmann, M. K. Weikum, T. Akhter, D. Alesini, A. S. Alexandrova, M. P. Anania, N. E. Andreev, I. Andriyash, M. Artioli, A. Aschikhin, *et al.*, EuPRAXIA Conceptual Design Report, Eur. Phys. J. Spec. Top. **229**, 3675 (2020).

[14] Y. Gao, R. Liu, C.-W. Chang, S. Charyyev, J. Zhou, J.D. Bradley, T. Liu, and X. Yang A potential revolution in cancer treatment: A topical review of FLASH radiotherapy, J. Appl. Clin. Med. Phys. **23**, e13790 (2022).

[15] L. Labate, D. Palla, D. Panetta, F. Avella, F. Baffigi, F. Brandi, F. Di Martino, L. Fulgentini, A. Giulietti, P. Köster, *et al.*, Toward an effective use of laser-driven very high energy electrons for radiotherapy: Feasibility assessment of multi-field and intensity modulation irradiation schemes, Sci. Rep. **10**, 1 (2020).

[16] L. Karsch, E. Beyreuther, W. Enghardt, M. Gotz, U. Masood, U. Schramm, K. Zeil and J. Pawelke, Towards ion beam therapy based on laser plasma accelerators, Acta Onc. **56**, 1359 (2017).

[17] S.A.E. Johansson and T.B. Johansson Analytical application of particle induced X-ray emission, Nucl. Instr. Meth. **137**, 473 (1976).

[18] *Particle-Induced X-Ray Emission Spectrometry (PIXE)*, edited by S.A.E. Johansson, J.L. Campbell, and K.G. Malmqvist (Wiley, New York, 1995).

[19] *Atomic and Nuclear Analytical Methods XRF, Mössbauer, XPS, NAA and Ion-Beam Spectroscopic Techniques*, H.R. Verma (Springer-Verlag, Berlin Heidelberg 2007).

[20] M.R.J. Palosaari, M. Käyhkö, K.M. Kinnunen, M. Laitinen, J. Julin, J. Malm, T. Sajavaara, W.B. Doriese, J. Fowler, C. Reintsema, *et al.*, Broadband Ultrahigh-Resolution Spectroscopy of Particle-Induced X Rays: Extending the Limits of Nondestructive Analysis, Phys. Rev. Appl. **6**, 024002 (2016).

[21] F. Lucarelli, G. Calzolai, M. Chiari, M. Giannoni, D. Mochi, S. Nava, and L. Carraresi, The upgraded external-beam PIXE/PIGE set-up at LABEC for very fast measurements on aerosol samples, Nucl. Instrum. Methods Phys. Res. B **318**, 55 (2014).

[22] F. Lucarelli, G. Calzolai, M. Chiari, S. Nava, and L. Carraresi, Study of atmospheric aerosols by IBA techniques: The LABEC experience, Nucl. Instrum. Methods Phys. Res. B **417**, 121 (2018).

[23] E.T. William, Pixe analysis with external beams: systems and applications, Nucl. Instrum. Methods Phys. Res. B **3**, 211 (1984).

[24] K. Maeda, K. Hasegawa, H. Hamanaka, and K. Ogiwara, Development of an in-air high-resolution PIXE system, Nucl. Instrum. Methods Phys. Res. B **134**, 418 (1998).

[25] T. Sakai, M. Oikawa, T. Sato, T. Nagamine, H.D. Moon, K. Nakazato, and K. Suzuki, New in-air micro-PIXE system for biological applications, Nucl. Instrum. Methods Phys. Res. B **231**, 112 (2005).

[26] M. Menu, External beam applications to painting materials, Nucl. Instrum. Methods Phys. Res. B **75**, 469 (1993).

[27] M. Chiari, External Beam IBA Measurements for Cultural Heritage, Appl. Sci. **13**, 3366 (2023).

[28] F. Taccetti, L. Castelli, M. Chiari, C. Czelusniak, S. Falciano, M. Fedi, F. Giambi, P. A. Mandò, M. Manetti, M. Massi, *et al.*, MACHINA, the Movable Accelerator for Cultural Heritage In-situ Non-destructive Analysis:

project overview, Rend. Lincei Sci. Fis. **34**, 427 (2023).

[29] A. Maffini, F. Mirani, M Galbiati, K. Ambrogioni, F. Gatti, M.S.G. De Magistris, D. Vavassori, D. Orecchia, D. Dellasega, V. Russo, *et al.*, Towards compact laser-driven accelerators: exploring the potential of advanced double-layer targets, EPJ Tech. Instrum. **10**, 15 (2023).

[30] F. Mirani, A. Maffini, and M. Passoni, Laser-Driven Neutron Generation with Near-Critical Targets and Application to Materials Characterization, Phys. Rev. Appl. **19**, 044020 (2023).

[31] M. Barberio and P. Antici, Laser-PIXE using laser-accelerated proton beams, Sci. Rep. **9**, 6855 (2019).

[32] M. Passoni, F.M. Arioli, L. Cialfi, D. Dellasega, L. Fedeli, A. Formenti, A.C. Giovannelli, A. Maffini, F. Mirani, A. Pazzaglia, *et al.*, Advanced laser-driven ion sources and their applications in materials and nuclear science, Plasma Phys. Control. Fusion **62**, 014022 (2020).

[33] M. Passoni, L. Fedeli, and F. Mirani, Superintense laser-driven ion beam analysis, Sci. Rep. **9**, 9202 (2019).

[34] F. Boivin, S. Vallières, S. Fourmaux, S. Payeur, and P. Antici, Quantitative laser-based x-ray fluorescence and particle-induced x-ray emission, New J. Phys. **24**, 053018 (2022).

[35] P. Puyuelo-Valdes, S. Vallières, M. Salvadori, S. Fourmaux, S. Payeur, J.-C. Kieffer, F. Hannachi, and P. Antici Combined laser-based X-ray fluorescence and particle-induced X-ray emission for versatile multi-element analysis, Sci. Rep. **11**, 9998 (2021).

[36] F. Mirani, A. Maffini, F. Casamichiela, A. Pazzaglia, A. Formenti, D. Dellasega, V. Russo, D. Vavassori, D. Bortot, M. Huault, *et al.*, Integrated quantitative PIXE analysis and EDX spectroscopy using a laser-driven particle source, Sci. Adv. **7**, eabc8660 (2021).

[37] L.A. Gizzi, L. Labate, F. Baffigi, F. Brandi, G. Bussolino, L. Fulgentini, P. Koester, and D. Palla, Overview and specifications of laser and target areas at the Intense Laser Irradiation Laboratory, High Power Laser Sci. Eng. **9**, E10 (2021).

[38] J. Bin, L. Obst-Huebl, J.-H. Mao, K. Nakamura, L.D. Geulig, H. Chang, Q. Ji, L. He, J. De Chant, Z. Kober, *et al.*, A new platform for ultra-high dose rate radiobiological research using the BELLA PW laser proton beamline, Sci. Rep. **12**, 1484 (2022).

[39] N. Xu, M.J.V. Streeter, O.C. Ettlinger, H. Ahmed, S. Astbury, M. Borghesi, N. Bourgeois, C.B. Curry, S.J.D. Dann, N.P. Dover, *et al.*, Versatile tape-drive target for high-repetition-rate laser-driven proton acceleration, High Power Laser Sci. Eng. **11**, e23 (2023).

[40] A.Groza, A. Chirosca, E. Stancu, B. Butoi, M. Serbanescu, D.B. Dreghici, and M. Ganciu Assessment of Angular Spectral Distributions of Laser Accelerated Particles for Simulation of Radiation Dose Map in Target Normal Sheath Acceleration Regime of High Power Laser-Thin Solid Target Interaction—Comparison with Experiments, Appl. Sci. **10**, 4390 (2020).

[41] A. Mancic, J. Robiche, P. Antici, P. Audebert, C. Blancard, P. Combis, F. Dorchies, G. Faussurier, S. Fourmaux, M. Harmand, *et al.*, Isochoric heating of solids by laser-accelerated protons: Experimental characterization and self-consistent hydrodynamic modeling, High Ener. Dens. Phys. **6**, 21 (2010).

[42] J. Fuchs, P. Antici, E. d'Humières, E. Lefebvre, M. Borghesi, E. Brambrink, C.A. Cecchetti, M. Kaluza, V. Malka, M. Manclossi, *et al.*, Laser-driven proton scaling laws and new paths towards energy increase, Nat. Phys. **2**, 48 (2006).

[43] T.F. Rösch, Z. Szabò, D. Haffa, J. Bin, S. Brunner, F.S. Engibrecht, A.A. Friedl, Y. Gao, J. Hartmann, P. Hilz, *et al.*, A feasibility study of zebrafish embryo irradiation with laser-accelerated protons Rev. Sci. Instrum. **91**, 063303 (2020).

[44] M. Nishiuchi, I. Daito, M. Ikegami, H. Daido, M. Mori, S. Orimo, K. Ogura, A. Sagisaka, A. Yogo, A.S. Pirozhkov, *et al.*, Focusing and spectral enhancement of a repetition-rated, laser-driven, divergent multi-MeV proton beam using permanent quadrupole magnets, Appl. Phys. Lett. **94**, 061107 (2009).

[45] G.A.P. Cirrone, G. Cuttone, F. Romano, F. Schillaci, V. Scuderi, A. Amato, G. Candiano, M. Costa, G. Gallo, G. Larosa, *et al.*, Design and Status of the ELIMED Beam Line for Laser-Driven Ion Beams, Appl. Sci. **5**, 427 (2015).

[46] S. Agostinelli, J. Allison, K.Amako, J.Apostolakis, H.Araujo P.Arce, M.Asai D.Axen, S.Banerjee, G.Barrand, *et al.*, Geant4 - A simulation toolkit, Nucl. Instrum. Meth. Phys. Res. A **506**, 250 (2003).

[47] J. Allison, K. Amako, J.Apostolakis, P.Arce, M.Asai, T.Aso, E.Bagli, A.Bagulya, S.Banerjee, G.Barrand, *et al.*, Recent developments in Geant4, Nucl. Instrum. Meth. Phys. Res. A **835**, 186 (2016).

[48] F. Brandi, L. Labate, D. Palla, S. Kumar, L. Fulgentini, P. Koester, F. Baffigi, M. Chiari, D. Panetta, and L.A. Gizzi, A Few MeV Laser-Plasma Accelerated Proton Beam in Air Collimated Using Compact Permanent Quadrupole Magnets Appl. Sci. **11**, 6358 (2021).

[49] L. Labate, A. Giulietti, D. Giulietti, P. Köster, T. Levato, L.A. Gizzi, F. Zamponi, A. Lübcke, T. Kämpfer, *et al.*, Novel x-ray multispectral imaging of ultraintense laser plasmas by a single-photon charge coupled device based pinhole camera, Rev. Sci. Instrum. **78**, 103506 (2007)

[50] L. Labate *et al.*, A laser-plasma source for CCD calibration in the soft X-ray range, Nucl. Instr. Meth. Phys. Res. A **495**, 148 (2002).

[51] A. Macchi, A superintense laser-plasma interaction theory primer, Springer (2013).

[52] S. Tudisco, C. Altana, G. Lanzalone, A. Muoio, G.A.P. Cirrone, D. Mascali, F. Schillaci, F. Brandi, G. Cristoforetti, P. Ferrara, *et al.*, Investigation on target normal sheath acceleration through measurements of ions energy distribution Rev. Sci. Instrum. **87**, 02A909 (2016).

[53] L.A. Gizzi, F. Baffigi, F. Brandi, G. Bussolino, G. Cristoforetti, A. Fazzi, L. Fulgentini, D. Giove, P. Koester, L. Labate, *et al.*, Light Ion Accelerating Line (L3IA): Test experiment at ILIL-PW Nucl. Inst. Meth. Phys. Res. A **909**, 160 (2018).

[54] F.J. Ziegler, M.D. Ziegler, and J.P. Biersack, SRIM – The stopping and range of ions in matter (2010) Nucl. Instrum. Meth. Phys. Res. B **268**, 1818 (2010); http://www.srim.org/.

[55] H. Paul and J. Sacher, Fitted empirical reference cross sections for K-shell ionization by protons, Atom. Data Nucl. Data Tables, **42**, 105 (1989).

[56] S. Aljboor, A. Angyal, D. Baranyai, E. Papp, M. Szarka, Z. Szikszai, I. Rajta, I. Vajda, and Z. Kertesz, Light-element sensitive in-air millibeam PIXE setup for fast measurement of atmospheric aerosol samples, J. Anal. At. Spectrom. **38**, 57 (2023).